COBEM 2021 26th International Congress of Mechanical Engineering
November 22-26, 2021, Virtual Congress, Brazil
ABCM Associação Brasileira de Engenharia e Ciências Mecânicas

COB-2021-2270
TEMPERATURE AND PRESSURE SENSITIVITY OF THE LAMINAR FLAME SPEED OF DIISOBUTYLENE/AIR MIXTURES

Christian de Araujo
Jônatas Vicente
Amir Antônio Martins de Oliveira Jr.
Combustion and Thermal Systems Engineering Laboratory, Department of Mechanical Engineering, Technology Center, Federal University of Santa Catarina - LabCET/EMC/CTC/UFSC, Campus João David Ferreira Lima, Trindade, Florianópolis, SC, Brazil.
eng.chrisaraujo@gmail.com, jonatas.vicente@labcet.ufsc.br, amir.oliveira@gmail.com

Ana Carolina Bueno Bontorin
Anderson Rouge dos Santos
CENPES - Centro de Pesquisas e Desenvolvimento Leopoldo A. M. de Mello, Cidade Universitária, Rio de Janeiro, RJ, Brazil.
ana.bontorin@petrobras.com.br, andersonrouge@petrobras.com.br

Abstract. *Diisobutylene is a hydrocarbon containing two isomers, 2,4,4-trimethyl-1-pentene and 2,4,4-trimethyl-2-pentene, which is representative of the branched alkenes gasoline, and to elucidate its role as an octane rating booster it is important to evaluate its combustion characteristics like laminar flame speed (LFS). The present study aims to investigate the influence of temperature, pressure, and equivalence ratio on the LFS of diisobutylene/air mixtures. Measurements were obtained in a constant volume reactor (CVR) for initial temperatures of T_u = 420 and 460 K, initial pressures of p_u = 1, 1.5, and 2 bar, and equivalence ratios of ϕ = 0.7 up to ϕ = 1.4. The results presents highest LFS value for the conditions evaluated was observed for equivalence ratio of ϕ = 1.0 and ϕ = 1.1. The increase in temperature presented an average increase in the LFS for the fuels of S_L = 8.7 cm/s, on the other hand, the increase of p = 0.5 bar in the base scenario presented a decrease at the LFS of S_L = 4.2 cm/s, and an increase of p = 1 bar presented a decrease of S_L = 6.7 cm/s. The conclusions of this work rely on the influence of the temperature and pressure in the LFS. The increase in temperature results in higher values of LFS, and an increase in pressure results in the opposite, reducing the LFS. Through this work, global equations for the fuels were obtained with good agreement with the experimental results.*

Keywords: *Diisobutylene, Antiknock additive, Laminar flame speed, Constant volume reactor, Primary reference fuels.*

1. INTRODUCTION

The range of alternative fuels available or under development, generally showing considerable variation in their chemical compositions, has renewed the interest in the measurement methods for laminar flame speed (LFS). Laminar flame speed is a main physical-chemical characteristic of the fuel-oxidant mixtures. It affects heat release, flammability limits, flame stability, and emissions, (Law, 2010). One of the interests of the LFS measurement is to obtain reliable data to test and improve the chemical kinetics mechanisms available, besides to characterize the behavior of the burning characteristics and compose a more consistent database regarding the fuel, (Coelho, 2014).

Due to the complexity of the combustion phenomena, there are difficulties regarding controlling and standardizing the basic experiments for measure the LFS, including correlations methodologies. These controls seek to ensure, among others, completely laminar conditions, isolating secondary phenomena. Thus, there are limited experimental data for pure fuel components, surrogates, and commercial fuels consisting of many chemical species, such as gasoline. Data from experimental results are even scarcer for high temperature and pressure, which are typical conditions in internal combustion engines (ICE's), as an example.

In the automotive industry and engineering, the knowledge about the LFS provides the necessary information to estimate the rate of fuel consumption, efficiency, and gas emissions on ICE. The capacity for the precise measurement is also essential to the turbulent combustion modeling and chemical kinetics mechanisms validation for conventional and alternative fuels, and on the possibility to use simplified models for the combustion on ICE's modeling, besides to the comprehension about the combustion phenomena in high pressure and temperature, (Varea *et al.*, 2012).

An important additive used to increase antiknock resistance and performance of gasoline is the Diisobutylene (DIB), which is one such high-performing hydrocarbon containing two isomers, 2,4,4-trimethyl-1-pentene (α-DIB - JC_8H_{16}) and 2,4,4-trimethyl-2-pentene (β-DIB - IC_8H_{16}), a representative of the branched alkenes gasoline, with a molecular formulation as C_8H_{16}, (Yin *et al.*, 2019). To elucidate its role as an octane rating booster it is important to evaluate its

combustion characteristics like laminar flame speed, thus allowing improved formulations for real fuels and surrogates.

The present study aims to investigate the influence of temperature, pressure, and equivalence ratio on the laminar flame speed of diisobutylene/air mixtures. Measurements of LFS were obtained in a constant volume reactor (CVR) for different conditions, being initial temperatures of 420 and 460 K, initial pressures of 1, 1.5, and 2 bar, and equivalence ratios from $\phi = 0.7$ to $\phi = 1.4$. These sets of temperatures and pressures allow understanding the temperature and pressure influence on diisobutylene LFS and comparison with literature data for n-heptane and iso-octane, which are the reference species for octane rating, as well as gasoline surrogates. Besides, a study developed by Kaiser *et al.* (1993), evaluating the gas emissions of an ICE with two fuels, pure diisobutylene and a surrogate of gasoline and diisobutylene, presented similarities in the gas emissions between the combustion of diisobutylene and iso-octane, which enhances the comparison with these primary reference fuels (PRF's).

2. EQUIPMENT AND MEASUREMENT PRINCIPLE OF LAMINAR FLAME SPEED

2.1 Experiment and data treatment

Figure 1 presents the experimental apparatus developed by (Hartmann, 2014; Monteiro, 2015). The CVR consists of two stainless-steel hemispheres that form a sphere with a diameter of utmost 300 mm and a volume of 14.8 liters. The windows are made of quartz and have a diameter of 190 mm, which after attached to the reactor with a flange permits the view of a diameter of 150 mm. They are mounted parallel to each other, one in each hemisphere. The CVR is instrumented with thermocouples K type at the wall and at an internal position 75 mm from the center, static and dynamic pressure sensors, injection septum, spark plugs, and filling/emptying piping systems. The heating system provides a maximum power of 1200 W. The test procedure is described in detail by Monteiro (2015).

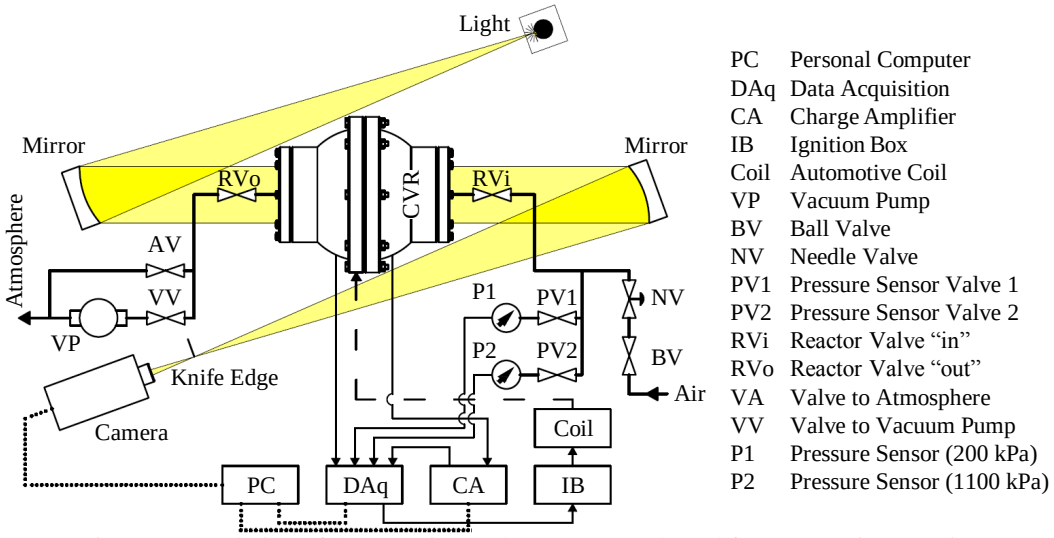

Figure 1: Rendering of the experimental apparatus. Adapted from Monteiro (2015).

The flame visualization is based in the Schlieren method, where the basic configuration consists of a punctual light source, mirrors and/or lens, and a high speed camera. The method uses the refraction index gradient in a flux, induced by the temperature gradient, (Settles, 2001). The CVR installed at the LabCET uses the Schlieren method Z type, which uses two oppositely tilted parabolic concave mirrors.

Figure 2 presents typical radius and pressure versus time measured in the reactor for a mixture of iso-octane and air, at equivalence ratio ϕ = 1.002, unburned pressure p_u = 100.1 kPa, unburned temperature T_u = 398.3 K. The mass of iso-octane injected in this condition is m_f = 0.8479 g. The measured laminar flame velocity is S_L = 52.40 cm/s and the burned Markenstein length is L_b = 1.017 mm (Monteiro, 2015).

Given the final measured values of laminar flame speed S_L obtained for a given fuel/air mixture, they are usually correlated to equivalence ratio ϕ, unburned pressure p_u, and unburned temperature T_u, using different semi-empiric equations. Metghalchi and Keck (1982) developed a series of experiments and proposes a flame speed correlation in the form of Eq. (1), which presented a remarkable agreement with results and has wide application.

$$S_L = S_{L,ref} \left(\frac{T_u}{T_{ref}} \right)^{n_T} \left(\frac{p_u}{p_{ref}} \right)^{n_p} (1 - d_1 Y_{dil})^{d_2} \tag{1}$$

where, $S_{L,ref}(\phi, T_{ref}, p_{ref})$ is the reference LFS for a given fuel expressed as polynomial function at the reference temperature and pressure. The exponents n_T and n_p are adjusted by linear regression of experimental curves and expressed as

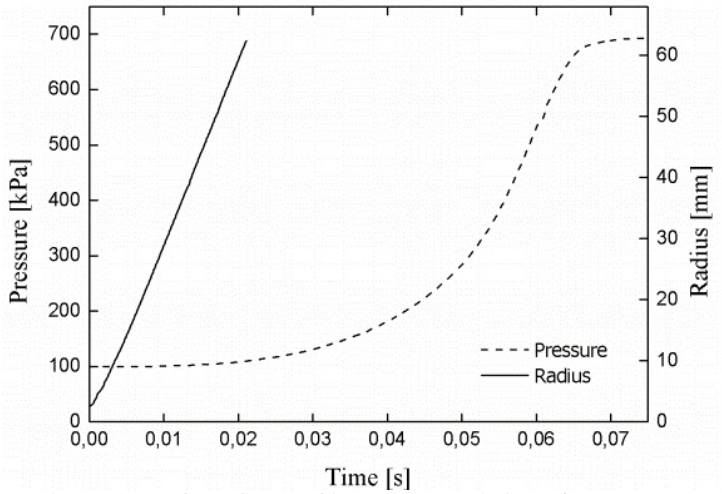

Figure 2: Flame radius R_F and pressure p for a flame of iso-octane and air at ϕ = 1,002, p_u= 100,1 kPa, and T_u = 398,3 K. The measured LFS is S_L = 52,40 cm/s and the burned Markenstein length is L_b = 1,017 mm. Monteiro (2015).

linear or quadratic functions of the equivalence ratio. In this equation, Y_{dil} is the mass fraction of an inert in the reactant fuel/air mixture, when there is no diluent in the fuel/air mixture, Y_{dil} = 0.

A study conducted by Monteiro (2015) on this CVR apparatus, evaluating the LFS of n-heptane, iso-octane, and other fuels, using five temperature levels: 298 K, 323 K, 348 K, 373 K, and 398 K and in each temperature level, six equivalence ratio levels from ϕ = 0.8 to ϕ = 1.3, resulted in the global fitting equation for these fuels based on the temperature and equivalence ratio.

The global equation for n-heptane is presented by Eq. (2) as follows

$$S_L(\phi, T_u) = (-152.59 + 409.35 \cdot \phi - 207.74 \cdot \phi^2 + 10.13 \cdot \phi^3) \left(\frac{T_u}{398}\right)^{(4.47 - 4.99 \cdot \phi + 2.10 \cdot \phi^2)} . \quad (2)$$

According to the author, using Eq. (4.6), the error associated will result in a deviation of $\pm$ 5% from the reference value for the LFS prediction of n-heptane.

In the same study, the previous author also developed a global equation to the LFS of iso-octane, the global fitting equation obtained is presented by Eq. (3) as

$$S_L(\phi, T_u) = (-88.73 + 211.26 \cdot \phi - 27.06 \cdot \phi^2 - 42.59 \cdot \phi^3) \left(\frac{T_u}{398}\right)^{(5.11 - 7.07 \cdot \phi + 3.51 \cdot \phi^2)} . \quad (3)$$

This equation will result in a deviation of $\pm$ 4% from the reference value,

These two equations presented by Monteiro (2013), can be compared with Eq. (1), being the $S_{L,ref}$ a cubic function at the reference temperature, and the exponent of temperature (n_T) a quadratic function, both based on the equivalence ratio. It can be observed that the equations do not present pressure dependence and dilution. The prediction of the LFS with them presents a good agreement to measurements in the entire flammability region, being these results presented and compared with data from the literature in his study.

The fittings of these global equations were obtained through the results obtained at the same experimental apparatus used in this work. These equations were used to estimate, compare and validate a set of previous tests developed with n-heptane, iso-octane at a temperature of 398 K, and pressure of 1 bar (temperature and pressure used in the fitting). Moreover, with the experimental results, a global equation was obtained following a similar procedure of fitting, obtaining an equation with the dependence of the pressure, and allowing to handle the tests performed at different pressures, and the comparison between the different fuels.

2.2 Outwardly propagating laminar premixed flame

Figure 3 presents a Schlieren image of a spherical, outwardly propagating, laminar, premixed flame and also a sector of the flame with the references o. The ignitors are positioned in the center of the reactor and at this time instant the flame surface has a radius R_F. The burned mixture occupies the region within the flame surface, at $r < R_F$, and the unburned mixture lays outside the flame surface, at $r > R_F$. In this figure, the velocities of the unburned and burned mixtures are u_u and u_b, and the unburned and burned flame speeds are S_u and S_b, respectively. All velocities are assumed normal to the flame surface.

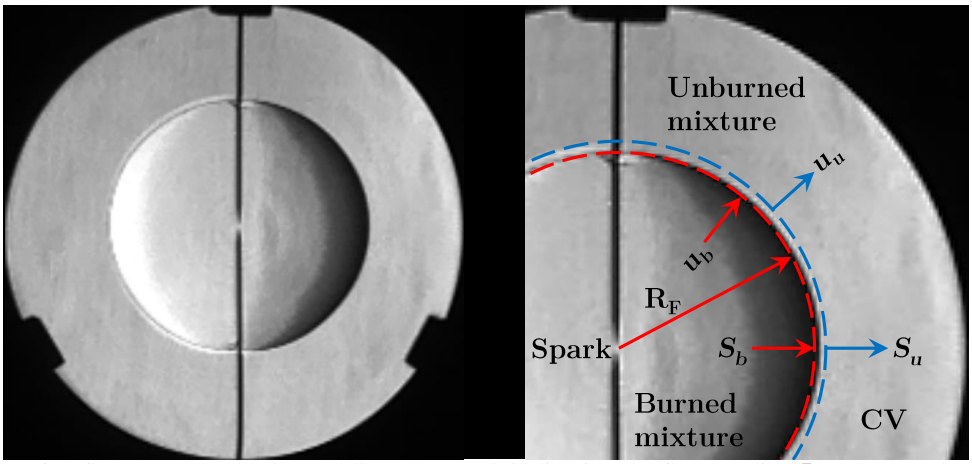

Figure 3: Propagating flame observed using Schlieren method, indicating the flame radius R_F, the speeds of the unburned and burned mixtures u_u and u_b normal to the flame sheet, and the unburned and burned flame speeds S_u and S_b.

In a plane, stationary, laminar premixed flame, the laminar flame speed S_L is equal to the flame consumption speed, i.e., the speed in which the reactant mixture is consumed in the flame. It is also equal to the flame displacement speed, i.e., the speed in which the unburned fuel mixture moves towards the flame. This is not true for the outwardly expanding (transient) flame.

For the transient, outwardly expanding flame, the speed of the moving flame front measured in respect to a coordinate system fixed in the center of the spherical reactor, named flame displacement speed S_F , is determined from the time recording of the flame position R_F as in Eq. (4).

$$S_f = \frac{dR_f}{dt}, \tag{4}$$

An overall mass conservation over a control volume around the flame sheet (see Fig. 1) moving with speed S_F gives Eq. (5)

$$R_u^2 \rho_u (u_u - S_F) = R_b^2 \rho_b (u_b - S_F) \tag{5}$$

or Eq. (6),

$$R_u^2 \rho_u S_u = R_b^2 \rho_b S_b \tag{6}$$

where ρ_u and ρ_b are the density of the unburned and burned mixtures, and $u_u = [(u \cdot n)]_u$ and $u_b = [(u \cdot n)]_b$ are the speeds of the unburned and burned mixtures in respect to the coordinate system fixed in the center of the spherical reactor at positions R_u and R_b.

This kinematic description carries a number of ambiguities already noted before (Bonhomme *et al.*, 2013). Primarily, the flame position R_F is an artifact of the flame surface detection technique, in this case a Schlieren flame visualization technique. Secondly, the flame surface is not sharp, but has a flame thickness of the order of $\ell_T \sim \alpha / S_u$, where α is the thermal diffusivity. Therefore, the overall mass balance carries an ambiguity related to where the position of the flame surface is defined and where the variables ρ_u, ρ_b, u_u and u_b are measured.

Moreover, the unburned mixture speed u_u is formed by two components. One component is the *flame conversion speed* S_u, i.e., the speed in which the unburned mixture crosses the flame front as reactants are converted to products. The second component derives from the outward movement of the unburned mixture towards the reactor wall as a result of the expansion of the burned mixture downstream from the flame front.

Since the flame is initiated in the center of the reactor, the burned mixture is progressively compressed towards the center of the reactor as the flame moves outwardly. This results in an inward burned mixture speed u_b.

Bonhomme *et al.* (2013) proposed a mass balance approach. After some mathematical development and assumptions, the equation for the flame sheet speed is given by Eq. (7)

$$S_u = \frac{\rho_b}{\rho_u} \frac{dR_F}{dt} \quad , \text{ or, } \quad S_u = E \frac{dR_F}{dt} \, , \tag{7}$$

where $E = \rho_u / \rho_b$ is the expansion ratio.

In summary, the hypothesis defining the flame speed are:

1. The experimentally detected flame position R_F is the radius of the sphere that encompasses the entire mass of CO_2 at any given instant of time.
2. The mass concentration of CO_2, $\rho_b Y_{CO_{2,b}}$, is uniform within the burned mixture and zero in the unburned mixture region.
3. The position where the conversion velocity S_u is defined is the same as the experimentally detected flame position, $R_u = R_F$.

The speed of the outwardly propagating spherical flame is affected by flame stretch. In Eq. (8) the flame stretch rate $\mathcal{K}$ is defined as

$$\mathcal{K} = \frac{1}{A_F}\frac{dA_F}{dt}, \tag{8}$$

where A_F is the flame surface area. The flame stretch rate is a measure of the deformation of the flame surface resulting from its motion and the underlying hydrodynamic strain. In Eq. (9) for the outwardly propagating spherical flame, $A_F = 4\pi R_2^F$ and

$$\mathcal{K} = \frac{2}{R_F}\frac{dR_F}{dt}\,. \tag{9}$$

Thus, the outwardly propagating spherical flame is positively stretched, i.e., it is extended. For stretched flames, the laminar flame speed S_L has been related to the consumption speed S_u as in Eq. (10)

$$S_u = S_L - \mathcal{L}\mathcal{K}\,, \tag{10}$$

where $\mathcal{L}$ is the Markstein lenght. This equation is known as the linear model.

In a more comprehensive model, Kelley and Law (2009) presents the non-linear model by Eq. (11), where the laminar flame speed S_L has been related to the consumption speed S_u as

$$\left(\frac{S_u}{S_L}\right)^2 \ln\left(\frac{S_u}{S_L}\right)^2 = -\frac{2\mathcal{L}}{S_L}\mathcal{K}\,, \tag{11}$$

In summary, the method of measuring the laminar flame speed in a CVR consists in:
1. Measuring the R_F as a function of time t while the pressure increase remains below 10 % of the initial pressure p_u.
2. Extracting the time derivative of R_F, $\dot{R}_F = dR_F/dt$, using some smoothing technique.
3. Calculating the stretch rate $\mathcal{K} = 2\dot{R}_F/R_F$.
4. Calculating the flame speed in respect to the unburned mixture $S_u = \dot{R}_F/E$.
5. Curve fitting the linear model, Eq. (10), obtaining first estimates of S_L and $\mathcal{L}$.
6. Curve fitting the non-linear model, Eq. (10), obtaining the final estimates of S_L and $\mathcal{L}$.
7. Evaluating the statistical uncertainties in S_L and $\mathcal{L}$.

3. RESULTS

As previously mentioned, a diisobutylene/air mixture was selected for this study since it is of fundamental importance to evaluate the behavior of the pure component, being an important additive used to formulate surrogates of conventional gasoline, herewith n-heptane and iso-octane.

Figure 5 presents the values of laminar flame speed obtained through experimental measurements in the CVR equipment for n-heptane and iso-octane at T_u = 398 K and p_u = 1 bar for different equivalence ratios, varying from ϕ = 0.7 to ϕ = 1.4, the experimental results for both components are compared with the the LFS estimated by Eq. (2) and Eq. (3) presented by Monteiro (2015) and the experimental results obtained by Dirrenberger *et al.* (2014). Also presenting the errors of the measurements and the estimated errors using the fitted global equations (represented by the dashed lines in the figures).

The results of these previous tests presented a good agreement for both fuels, especially for iso-octane, which practically was located within the error range of the equation and close to the experimental results from Dirrenberger *et al.* (2014). For n-heptane there was a difference in the measurements for ϕ = 1.3, which was above the upper limit of the equation error and also the experimental results from the previously mentioned author, however, according to the equivalence ratio increase, the results of this study returns to a better agreement with the experimental result from Dirrenberger *et al.* (2014), and within the limits of the values predicted by the Eq. (2).

These tests were performed to analyze the behavior of the reactor and it was used to validate the alignment of the experimental apparatus as well the systems of temperature and pressure controls. With the validation, it was possible to perform the experiments proposed for this study, also, to obtain and use of the equations to predict and make possible the comparison between the results of the fuels.

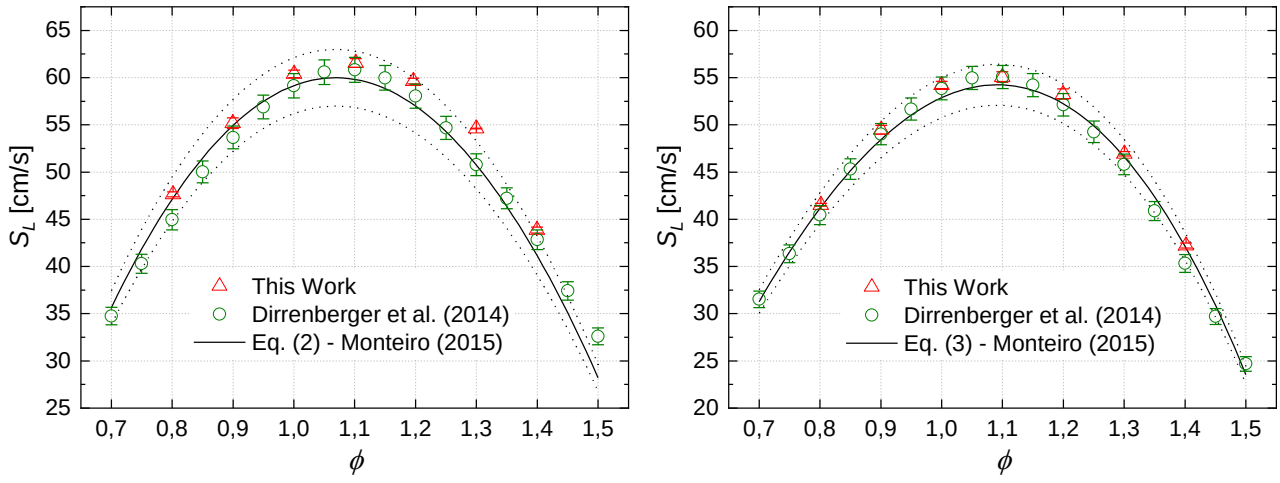

(a) (b)

Figure 4: Comparison of the LFS versus equivalence ratio of n-heptane and iso-octane/air mixtures, Fig. 4a and 4b respectively, for temperature of T = 398 K and pressure p = 1 bar, comparing the results from this work with data from the literature.

With the experimental results obtained for n-heptane, iso-octane, and diisobutylene/air mixtures a fitting was performed and as a results, the global equations for these species with dependence of temperature, pressure and equivalence ratio are presented here by Eq. 12, Eq. 13, and Eq. 14, for each specie respectively, as follow

$$S_L(\phi, T_u, p_u) = (-100.9 + 232.6\cdot\phi - 22.1\cdot\phi^2 - 51.2\cdot\phi^3)\left(\frac{T_u}{420}\right)^{(5.36-6.79\cdot\phi+3.02\cdot\phi^2)}\left(\frac{p_u}{1}\right)^{(-0.73+1.0\cdot\phi-0.47\cdot\phi^2)}, \quad (12)$$

$$S_L(\phi, T_u, p_u) = (-127.0 + 328.58\cdot\phi - 115.9\cdot\phi^2 - 20.3\cdot\phi^3)\left(\frac{T_u}{420}\right)^{(6.88-10.64\cdot\phi+5.18\cdot\phi^2)}\left(\frac{p_u}{1}\right)^{(-0.84+1.72\cdot\phi-1.0\cdot\phi^2)}, \quad (13)$$

$$S_L(\phi, T_u, p_u) = (-83.5 + 186.29\cdot\phi + 19.48\cdot\phi^2 - 62.0\cdot\phi^3)\left(\frac{T_u}{420}\right)^{(5.74-6.96\cdot\phi+2.86\cdot\phi^2)}\left(\frac{p_u}{1}\right)^{(-0.25+0.42\cdot\phi-0.33\cdot\phi^2)}. \quad (14)$$

The equations for N-Heptane (Eq. Eq. 12), and for Iso-Octane (Eq. Eq. 13) presents a deviation of $\pm$ 3.5% and $\pm$ 4.5%, respectively, on the prediction based on the experimental results. Furthermore, the equation for the Diisobutylene (Eq. Eq. 14) presents a deviation of $\pm$ 3.5% on the prediction of the LFS based on the experimental results.

Figure 5 presents the experimental values for the laminar flame speed of diisobutylene - n-heptane/air (Fig. 5a and 5c), and diisobutylene - iso-octane/air mixtures (Figure 5b and 5d) for a fixed pressure of p_u = 1 bar, at the temperature conditions of T_u = 420 K and T_u = 460 K for different equivalence ratios, varying from ϕ = 0.7 to ϕ = 1.4, the experimental results are also compared with the the LFS estimated by Eq. 12, Eq. 13, and Eq. 14.

Results show that the highest LFS value for T = 420 K, p = 1 bar (Fig. 5a and 5c) was observed for the equivalence ratio of ϕ = 1.1 for the three fuels, with an average value of S_L = 63 cm/s for diisobutylene, S_L = 67.2 cm/s for n-heptane, and S_L = 59.6 cm/s for iso-octane. Comparisons with n-heptane and iso-octane data show that LFS values for diisobutylene from ϕ = 0.8 to ϕ = 1.4 is consistently lower than that of n-heptane, approximately S_L = 5 cm/s, at ϕ = 0.7 this difference is approximately S_L = 3 cm/s. The upper limit of the predicted values for diisobutylene is near of the lower limit of the equation for n-heptane. In comparison with the other component, the results of diisobutylene are higher than those of iso-octane, an average of S_L = 1.5 cm/s for ϕ = 0.8, S_L = 3 cm/s for ϕ = 0.8 to ϕ = 1.2, and S_L = 4 cm/s for ϕ = 1.3 and ϕ = 1.4. The lower limit of the diisobutylene equation (Eq. 14) practically coincides with the central values obtained with the iso-octane equation (Eq. 13). Similar behavior is observed with the upper limit of the iso-octane equation and the diisobutylene center values.

For the temperature condition of T_u = 460 K (Figure 5b and 5d) there was no evaluate all the equivalence ratios presented previously, due to the availability of fuel and the fact that the central and lateral values may show the tendency of the flame speed behavior in this condition. Evaluating the values obtained in this condition, it is observed an increase in LFS, an average value of S_L = 9 cm/s for the three fuels. Significant differences in the LFS increase were not observed between them.

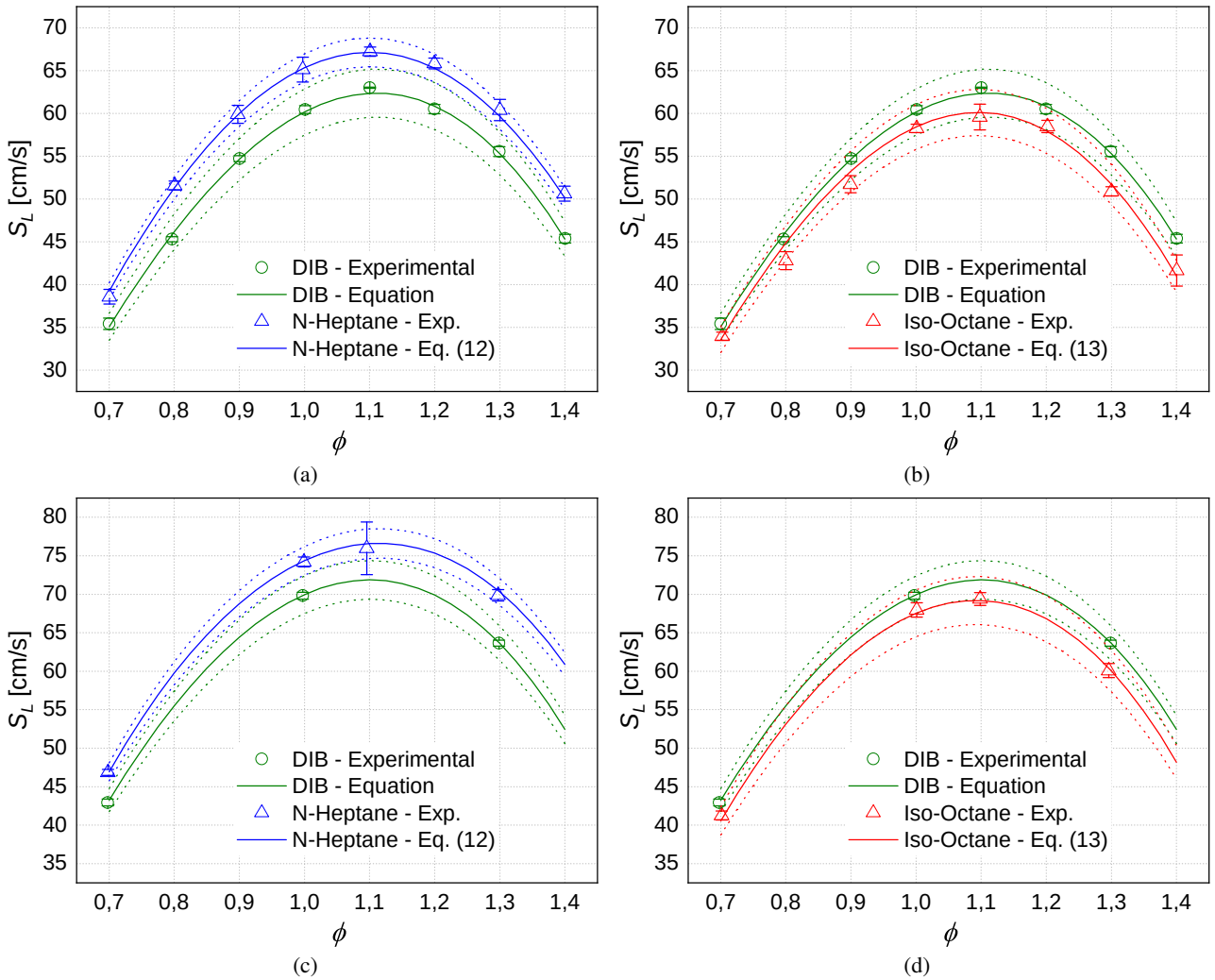

Figure 5: Comparison of the LFS versus equivalence ratio for a fixed pressure of p = 1 bar at a temperature of T = 420 K, Fig. (5a) and (5b), and temperature of T = 460 K, Fig. (5c) and (5d), for n-heptane and iso-octane - diisobutylene/air mixtures.

Figure 6 presents the experimental and predicted values for the laminar flame speed of diisobutylene - n-heptane/air (Fig. 6a and 6c), and diisobutylene - iso-octane/air mixtures (Figure 6b and 6d) for a fixed temperature of T_u = 420 K, at pressure conditions of p_u = 1.5 bar and p_u = 2.0 bar for different equivalence ratios, varying from ϕ = 0.7 to ϕ = 1.4.

Results show that the increase in pressure reduces all the LFS in this condition of temperature of T_u = 420 K and pressures. For the pressure of p_u = 1.5 bar (Fig. 6a and 6b) the highest LFS values was also observed for the equivalence ratio of ϕ = 1.1 for the three fuels, with an average value of S_L = 57.3 cm/s for diisobutylene, S_L = 62.2 cm/s for n-heptane, and S_L = 56.8 cm/s for iso-octane. The increase in pressure results in an average reduction of the LFS for diisobutylene of S_L = 4.3 cm/s, for n-heptane this reduction is S_L = 5.4 cm/s, and for iso-octane S_L = 3 cm/s. Moreover, it can be observed that the LFS for n-heptane at ϕ = 1.3 is near of the result for diisobutylene comparing with the results presented in Fig. 5, for iso-octane the pattern has remained the same.

For the pressure of p_u = 2.0 bar (Fig. 6c and 6d) there was no experimental results for n-heptane due to a problem with the workbench, for diisobutylene and iso-octane, the highest LFS values was observed for the equivalence ratio of ϕ = 1.0 for diisobutylene and ϕ = 1.1 for iso-octane, with an average value of S_L = 54.6 cm/s for diisobutylene, and S_L = 51.4 cm/s for iso-octane. The increase of p = 1 bar in the initial pressure, being the base scenario as p_u = 1 bar, results in an average reduction of the LFS for diisobutylene of S_L = 6.5 cm/s, and for iso-octane S_L = 6.8 cm/s. For the three fuels, and both pressures presented previously, was observed that the reduction is smaller at lower equivalence ratios and reduce more as the equivalence ratio increases.

The LFS difference for n-heptane at the tests with T_u = 420 K, p_u = 1.5 bar at ϕ = 1.3 reflects in the predicted values using Eq. 12 for the condition of p_u = 2 bar, following the pattern and showing close LFS values between the two fuels. This difference is more evident because there are no experimental results to back up these predicted values, which results in no confidence in this prediction since the experimental data is used for the equation fitting.

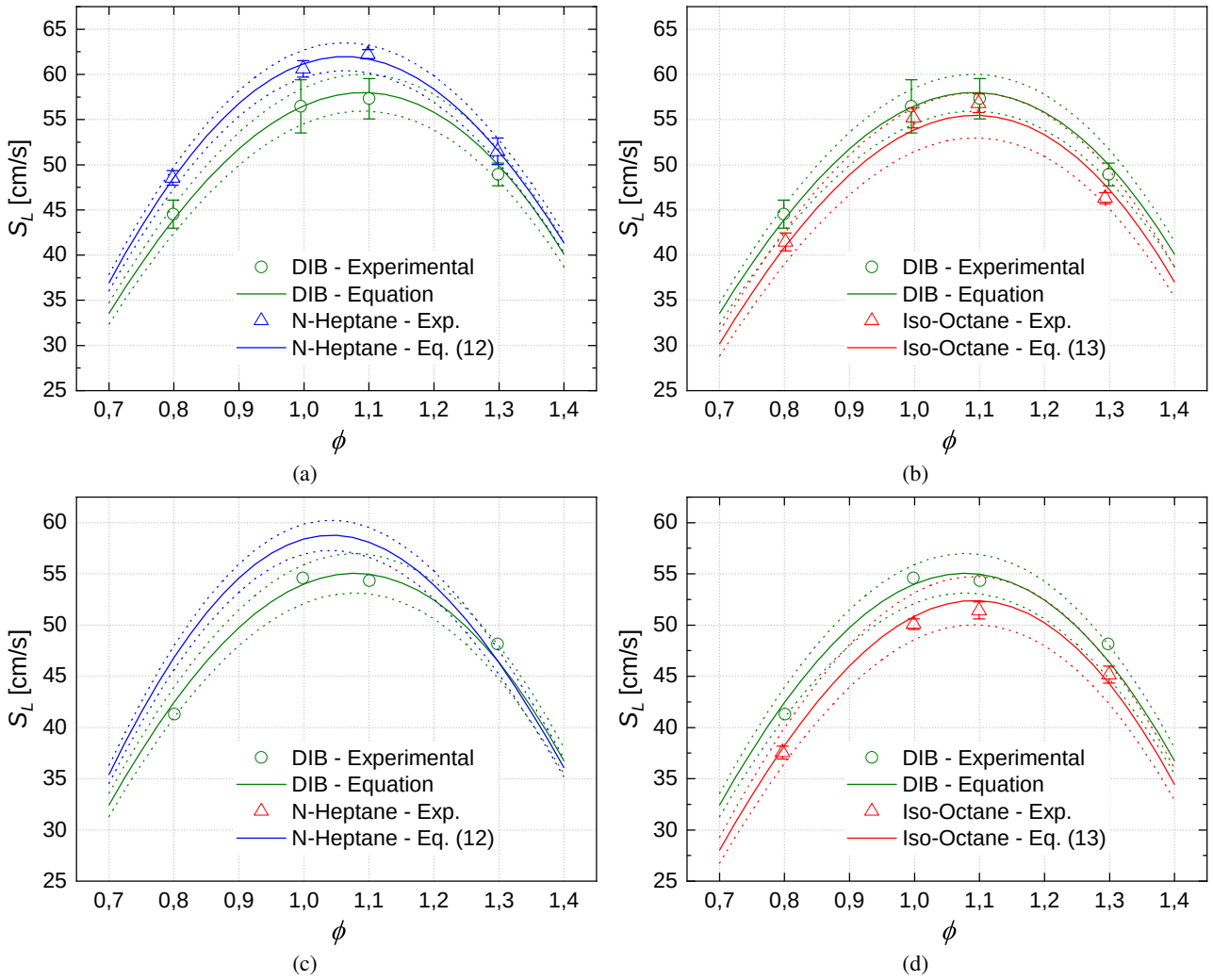

Figure 6: Comparison of the LFS versus equivalence ratio for a fixed temperature of T = 420 K at a pressure of p = 1.5 bar, Fig. (6a) and (6b), and pressure of p = 2 bar, Fig. (6c) and (6d), for n-heptane and iso-octane - diisobutylene/air mixtures.

Figure 7 presents the experimental and predicted values for the laminar flame speed of diisobutylene/air mixtures for a fixed temperature of T_u = 460 K for pressures of p_u = 1.5 bar and p_u = 2.0 bar, Fig. 7a and 7b, respectively.

Analyzing the results can be observed a good agreement of the experimental results with the predicted value at the pressure of p_u = 1.5 bar. For the pressure p_u = 2 bar the results at ϕ = 0.8 present a good agreement, at ϕ = 1.1 the result is coincident to the upper limit of the equation and in higher equivalence ratio, ϕ = 1.3, are above of this upper limit of the equation.

These tests were developed with no replication due to the availability of fuel. For a first analysis, the results were consistent with what was predicted by the equation. The authors expect to develop more tests in the future, to improve the equation coefficients and compare them with experimental results.

An important observation of the results based on the temperature and pressure sensibility of the laminar flame speed for all results presented here is that for a fixed pressure, the LFS increases with temperature since high temperatures increase the dissociation reactions that produce free radicals. These radicals initiate the combustion reaction, which is why the flame spread velocity increases, (Glassman *et al.*, 2014). Increasing the initial pressure at a fixed temperature leads to a decrease in the LFS. At high pressures, the recombination reaction $H + O_2 + M \rightarrow HO_2 + M$ reduces the concentration of the H atom and thus competes with the initial reaction by producing the free radicals O and OH through the following reaction $H + O_2 \rightarrow O + OH$. This process tends to reduce the overall oxidation rate and inhibit the combustion reaction. Thus, the flame speed decreases, (Glassman *et al.*, 2014).

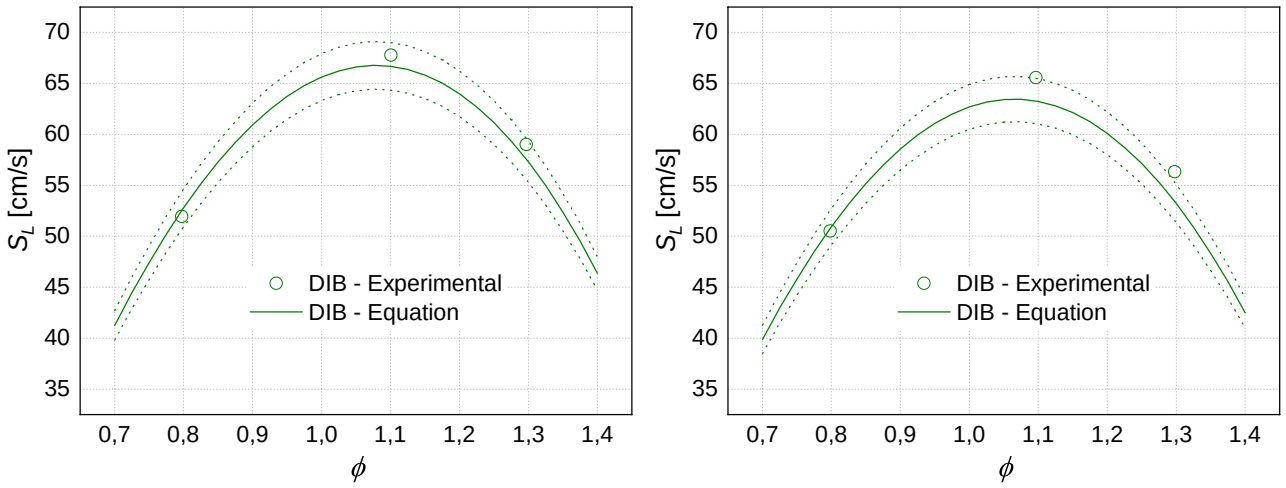

(a) (b)

Figure 7: Comparison of the LFS versus equivalence ratio for a fixed temperature of T = 460 K at a pressure of p = 1.5 bar, Fig. (7a), and pressure of p = 2 bar, Fig. (7b), for diisobutylene/air mixtures.

4. CONCLUSIONS

The present study investigates the influence of temperature, pressure, and equivalence ratio on the laminar flame speed of diisobutylene/air mixtures through measurements of LFS in a constant volume reactor for different conditions. Furthermore, a comparison with the LFS results with the primary reference fuels was also presented.

The preliminary tests with the PRFs showed consistency with the results presented in the literature and results obtained in this same experimental apparatus in another study.

The experimental results showed that for a fixed pressure, increasing temperature causes an increase in laminar flame speed, reflecting the influence of temperature on this parameter, presenting a similar change among the fuels evaluated. For the tests with a fixed temperature and varying pressure, it was observed that increasing the pressure results in lower LFS values. The tests reflected the sensitivity of LFS to the variation of these parameters.

Global equations for diisobutylene, n-heptane, and iso-octane/air mixtures without dilution were obtained as a function of temperature, pressure, and equivalence ratio. The equations presented a good agreement with the experimental results. Moreover, the predicted values of LFS using the global equation for diisobutylene/air mixtures, in different conditions than those used for the equation fitting, were compared with experimental results at these conditions, which presented a good agreement between them.

For future work, the authors hope to investigate other equivalence ratios under the same conditions of this work, intended to improve the database with more points under these conditions. In addition, the use of more experimental data will enhance the fitting of the global equations. Moreover, one can seek other ways to refine the exponential coefficients of temperature and pressure to predict the LFS at different conditions for validation and internal combustion engine operating conditions, also evaluate the use of other correlations for laminar flame speed.

5. ACKNOWLEDGEMENTS

The authors thank CENPES-Petrobras for supplying the fuels. The second author thanks the financial support from National Petroleum, Natural Gas and Biofuels Agency - ANP -, from Financier of Studies and Projects - FINEP - and the Ministry of Science, Technology and Innovation - MCTI through the ANP's Human Resources Program for the Oil and Gas Sector - PRH-ANP/MCTI.

6. REFERENCES

Bonhomme, A., Selle, L. and Poinsot, T., 2013. "Curvature and confinement effects for flame speed measurements in laminar spherical and cylindrical flames". *Combustion and Flame*, Vol. 160, No. 7, pp. 1208–1214.

Coelho, F.J.V.S., 2014. *Laminar flat flame speed measurement of methane-air and natural gas-air mixtures through heat flux method (in Portuguese)*. Master's thesis, Federal University of Rio Grande do Sul.

Dirrenberger, P., Glaude, P., Bounaceur, R., Le Gall, H., da Cruz, A.P., Konnov, A. and Battin-Leclerc, F., 2014. "Laminar burning velocity of gasolines with addition of ethanol". *Fuel*, Vol. 115, No. 1, pp. 162–169.

Glassman, I., Yetter, R.A. and Glumac, N.G., 2014. *Combustion*. Academic Press, 5th edition.

Hartmann, R.M., 2014. *Instrumentation and operacionalization of a constant volume reactor to measure laminar flame*

speed (in Portuguese). Master's thesis, Graduate Program in Mechanical Engineering, Federal University of Santa Catarina.

Kaiser, E.W., Siegl, W.O., Cotton, D.F. and Anderson, R.W., 1993. "Effect of fuel structure on emissions from a spark-ignited engine. 3. Olefinic fuels". *Environmental Science & Technology*, Vol. 27, No. 7, pp. 1440–1447.

Kelley, A. and Law, C., 2009. "Nonlinear effects in the extraction of laminar flame speeds from expanding spherical flames". *Combustion and Flame*, Vol. 156, No. 9, pp. 1844–1851.

Law, C.K., 2010. *Combustion Physics*. Cambridge University Press, 1st edition.

Metghalchi, M. and Keck, J.C., 1982. "Burning velocities of mixtures of air with methanol, isooctane, and indolene at high pressure and temperature". *Combustion and Flame*, Vol. 48, No. 1, pp. 191–210.

Monteiro, J.O.D., 2013. *Medição de Velocidade de Chama Laminar de Misturas de Gás Natural e Ar em Reator de Volume Constante*. Trabalho de conclusão de curso (graduação), Universidade Federal de Santa Catarina.

Monteiro, J.O.D., 2015. *Laminar Flame Speed of Fuel Mixtures Applied to Spark Ignition Internal Combustion Engines*. Master's thesis, Graduate Program in Mechanical Engineering, Federal University of Santa Catarina.

Settles, G., 2001. *Schlieren and Shadowgraph Techniques: Visualizing Phenomena in Transparent Media*. Springer-Verlag Berlin Heidelberg, 1st edition.

Varea, E., Modica, V., Vandel, A. and Renou, B., 2012. "Measurement of laminar burning velocity and Markstein length relative to fresh gases using a new postprocessing procedure: Application to laminar spherical flames for methane, ethanol and isooctane/air mixtures". *Combustion and Flame*, Vol. 159, No. 2, pp. 577–590.

Yin, G., Hu, E., Huang, S., Ku, J., Li, X., Xu, Z. and Huang, Z., 2019. "Experimental and kinetic study of diisobutylene isomers in laminar flames". *Energy*, Vol. 170, pp. 537–545.

7. RESPONSIBILITY NOTICE

The authors are solely responsible for the printed material included in this paper.